 

# *Headline Articles*

## Control of Molecular Orientation of $\alpha$-Helix in the Monolayer at Air–Water Interface

**Tomokiyo Doi, Takatoshi Kinoshita,* Yoshiharu Tsujita, and Hiroaki Yoshimizu**

Department of Materials Science and Engineering, Nagoya Institute of Technology, Gokiso-cho, Showa-ku, Nagoya 466-8555.

(Received August 18, 2000)

Amphiphilic block copolymers of poly(L-leucine-co-ethylene glycol) ($PLeu_m$–$PEG_n$) having three different compositions, $m:n$ = 80:23, 57:46, and 66:114, were prepared and spread at an air–water interface to form a stable monolayer. The $\alpha$-helical conformation of PLeu segment in the monolayers was confirmed by FT-IR and circular dichroism measurements. The molecular orientation of PLeu helix rods in the monolayer was estimated by surface pressure-area isotherm and FT-IR reflection absorption spectroscopy measurements. As a result, we confirmed that $\alpha$-helix rod of PLeu segment oriented slightly normal to the membrane plane. Furthermore, it was indicated that each $\alpha$-helical rod in the $PLeu_{57}$–$PEG_{46}$ monolayer is effectively oriented normal to the interface compared to that in the $PLeu_{80}$–$PEG_{23}$ and $PLeu_{66}$–$PEG_{114}$ monolayers.

The orientation of $\alpha$-helical segments in the membrane protein is essential to control their intelligent functions such as the transport of specific ions and/or the signal transductions.[1] In order to analysis and mimic these functions, it is important to control the orientation of $\alpha$-helix molecules in artificial membrane systems. Recently, a number of methods have been reported in order to control the orientation of $\alpha$-helix in the monolayer and Langmuir–Blodgett (LB) films. For example, the LB method gave a preferred the parallel orientation of $\alpha$-helices in the dipping direction.[2,3] Furthermore, in order to construct the polypeptide molecular membrane systems consisting of $\alpha$-helices oriented normal to the membrane plane, several techniques have been proposed.[4–14] We also reported a preparation method for the membrane having $\alpha$-helices oriented perpendicular to the membrane plane by the adsorption of the polypeptide having thiol group at the terminal to the Au(111) surface.[13] The Au surface could not completely be covered with the polypeptide monolayer by this adsorption method. On the other hand, we showed that an amphiphilic polypeptide, poly($\gamma$-methyl L-glutamate) containing hydrophilic $\beta$-cyclodextrin at the terminal of the molecule, was able to stand in the monolayer membrane at an hexane–water interface.[9,11] However, it is much easier to prepare the LB film by transferring the monolayer at air–water interface compared with that at oil–water interface.

In this study, in order to obtain a normal orientation of $\alpha$-helical rods in the monolayer at "air–water interface", we have prepared poly(L-leucine) containing polyethylene glycol (PEG) as a hydrophilic block segment and we have estimated the molecular orientation at the interface. The block copolymers, $PLeu_m$–$PEG_n$, formed a stable monolayer at air–water interface and the $\alpha$-helical rods of PLeu segment tend to stand at the interface by compression of the monolayer. Thus PEG segments are essential for standing of PLeu moieties by compression of the monolayer. Furthermore, we also discuss the influence of the difference in the composition, i.e., PLeu/PEG ratio, on the $\alpha$-helix orientation at the interface.

### Experimental

**Preparation of Amphiphilic Block Copolymers.** Amphiphilic block copolymers of poly(L-leucine-co-ethylene glycol) ($PLeu_m$–$PEG_n$) were prepared by polymerization of *N*-carboxyanhydride of L-leucine with polyethylene glycols ($M_w$ = 5050, 2050, 1050; NOF Corporation) having an amino group at a terminal of the chain as an initiator in benzene (Fig. 1). An average degree of polymerization of PLeu moiety was estimated by high-resolution $^1$H NMR measurements (Varian XL-200 spectrometer) of the sample in trifluoroacetic acid. Thus we obtained three samples of different composition, $PLeu_m$–$PEG_n$; $m:n$ = 80:23, 57:46, 66:114.

**Circular Dichroism (CD) Measurements.** CD measurements of the copolymers in hexafluoro-2-propanol (HFP) were carried out with a Jasco J-820K spectropolarimeter. CD spectra of the HFP solution of $PLeu_m$–$PEG_n$ were expressed in terms of molar ellipticity, $[\theta]$, based on the mean residue molecular weight. In order to confirm the secondary structure of PLeu segments in molecular

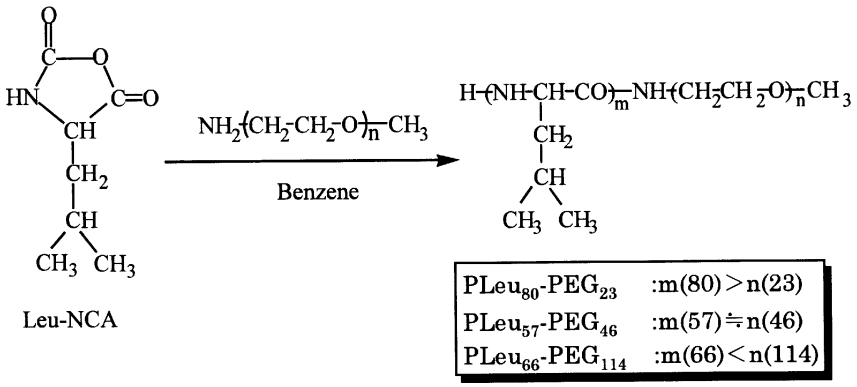


Fig. 1. Poly(L-leucine-co-ethylene glycol).

membrane, the CD spectra of LB film were also measured. In this case the CD spectra were expressed in ellipticity, $\theta$. The monolayer on the water was transferred onto the quartz plate by the horizontal lifting method at 25 mN m$^{-1}$ using a Langmuir–Blodgett film balance (Nippon Laser & Electronics Lab., NL-LB80-MT-M). We repeated this procedure five times to get LB film of PLeu$_m$–PEG$_n$ on the quartz plate.

**Surface Pressure-Area ($\pi$-A) Isotherms.** The surface pressure-area ($\pi$-A) isotherms of the copolymer monolayers were obtained by the Wilhelmy method using Langmuir–Blodgett film balance. The surface pressure was determined with a precision of 1.0 $\times$ 10$^{-4}$ N m$^{-1}$. A Teflon trough (90 mm $\times$ 160 mm $\times$ 2 mm) was filled with Milli-Q treated water. PLeu$_m$–PEG$_n$ was solved in the chloroform including 1% trifluoroacetic acid (TFA). The solution of PLeu$_m$–PEG$_n$ (1.0 $\times$ 10$^{-5}$ mol dm$^{-3}$) was spread onto the water surface by a microsyringe and the solvent was removed within 10 min to yield stable monolayer. The compression of the monolayer in the trough was carried out by moving the Teflon barrier by 2 mm min$^{-1}$.

**FT-IR Reflection Absorption Spectroscopy (FT-IR/RAS).** The spectrum of FT-IR/RAS was recorded on a Perkin Elmer Spectrum 2000 equipped with an MCT (Mercury–Cadmium–Telluride) detector with a resolution of 4 cm$^{-1}$. An attachment, FT 80 Specular Reflectance (Spectra-Tech Inc.), was used together with a polarizer (Graseby Specac Ltd.) to select the p-polarized light. For the FT-IR/RAS measurement, the monolayer at air–water interface was transferred onto the Au-coated glass plate by the vertical dipping method while keeping the surface pressure at $\pi$ = 25 mN m$^{-1}$ using Langmuir–Blodgett film balance (Nippon Laser & Electronics Lab., NL-LB240-MWA).

The tilt angle of $\alpha$-helical axis from the surface normal was calculated by the method proposed by Samulusky et al.[4]

$$\frac{A^{\mathrm{I}}{}_{\mathrm{obs}}}{A^{\mathrm{II}}{}_{\mathrm{obs}}} = K\frac{A^{\mathrm{I}}{}_{\mathrm{cal}}}{A^{\mathrm{II}}{}_{\mathrm{cal}}} \quad (1)$$

$$\frac{A^{\mathrm{I}}{}_{\mathrm{cal}}}{A^{\mathrm{II}}{}_{\mathrm{cal}}} = \frac{\{(\sin\gamma\sin 39^\circ)^2/2 + (\cos\gamma\cos 39^\circ)^2\}}{\{(\sin\gamma\sin 74^\circ)^2/2 + (\cos\gamma\cos 74^\circ)^2\}} \quad (2)$$

Here, $\gamma$ is an angle between the helix axis and the axis normal to the plane of the monolayer. $A^{\mathrm{I}}{}_{\mathrm{obs}}$ and $A^{\mathrm{II}}{}_{\mathrm{obs}}$ are the absorbance values of amide I and amide II, respectively, observed by FT-IR/RAS measurements. $A^{\mathrm{I}}{}_{\mathrm{cal}}/A^{\mathrm{II}}{}_{\mathrm{cal}}$ is the calculated ratio of absorbance. The value of $K$ was determined by Eq. 1 using the calculated value of $A^{\mathrm{I}}{}_{\mathrm{cal}}/A^{\mathrm{II}}{}_{\mathrm{cal}}$ when $\gamma$ = 90° in Eq. 2 and the ratio of the observed absorbance of the sample whose helices are oriented parallel to the Au substrate.

**Atomic Force Microscopy (AFM).** The LB films of PLeu$_m$–PEG$_n$ were observed by an atomic force microscope (Digital Instruments, Nanoscope III a). The measurement was performed in the tapping mode at room temperature with a silicon cantilever (Digital Instruments, NCH-10T). For the AFM observation, the monolayer on the water surface transferred to a freshly cleaved mica surface by the vertical dipping method while keeping the surface pressure at $\pi$ = 5 and 25 mN m$^{-1}$ using a Langmuir–Blodgett film balance (Nippon Laser & Electronics Lab., NL-LB240-MWA).

## Results and Discussion

**$\alpha$-Helical Structure of the PLeu Segment.** We estimated the structure of the PLeu segment by circular dichroism (CD) spectroscopy. The CD spectrum of the HFP solution of PLeu$_{57}$–PEG$_{46}$ is shown in Fig. 2a. The spectrum exhibited two negative bands at 208 and 222 nm typical of a right-handed $\alpha$-helix. From the value of $[\theta]_{222}$ (–3,2 $\times$ 10$^4$ deg cm$^2$ dmol$^{-1}$), we estimated that the $\alpha$-helix content[15] of PLeu$_{57}$–PEG$_{46}$ was 91% in the HFP solution. The CD spectrum of PLeu$_{66}$–PEG$_{114}$ was similar to that of PLeu$_{57}$–PEG$_{46}$, the $\alpha$-helix content was estimated to be 100%. PLeu$_{80}$–PEG$_{23}$ would not dissolve in HFP, so we could not estimate the $\alpha$-helix content. One may say, however, that the $\alpha$-helix structure of PLeu$_{80}$–PEG$_{23}$ is the most stable, for it has the highest Leu content among the three amphiphilic block copolymers. In order to estimate the conformation of PLeu segment in the molecular membrane, the CD spectrum of PLeu$_{57}$–PEG$_{46}$ LB (five layers) film is also shown in Fig. 2b. The accurate molecular ellipticity, $[\theta]$, could not be estimated owing to the linear dichroism of the film sample, so the CD spectrum of LB film was expressed in $\theta$ (mdeg). The $\alpha$-helical structure of PLeu segments can be confirmed from the CD pattern in the spectrum exhibiting two negative bands at 208 and 222 nm typical of a right-handed $\alpha$-helix. In addition, FT-IR spectrum of PLeu$_{57}$–PEG$_{46}$ LB (monolayer) film is shown in Fig. 3. It exhibited two bands at 1662 and 1545 cm$^{-1}$, assigned as Amide I and Amide II of the typical $\alpha$-helix,[10] respectively. Therefore, it seems that the PLeu segment exists as the $\alpha$-helical conformation in the LB film obtained by transfer-

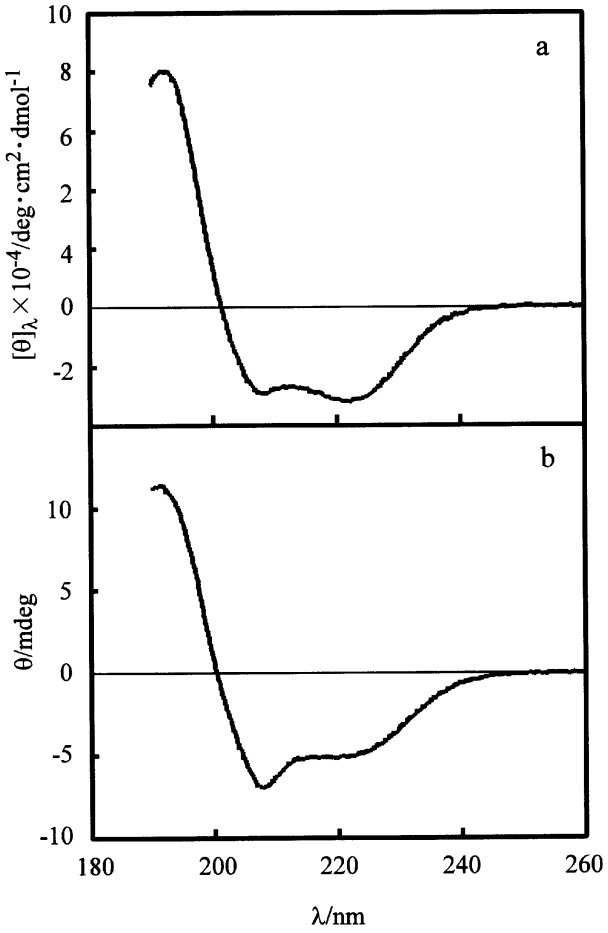


Fig. 2. Circular dichroism spectra of $PLeu_{57}$–$PEG_{46}$. a; HFP solution, b; LB film.

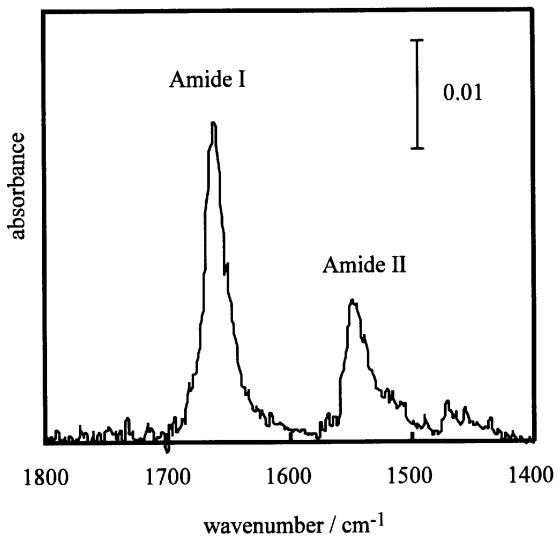


Fig. 3. FT-IR reflection absorption spectrum of monolayer of $PLeu_{57}$–$PEG_{46}$ transferred to a Au substrate.

ring the monolayer at 25 mN m$^{-1}$ from water surface. The PLeu segment in $PLeu_{80}$–$PEG_{23}$, $PLeu_{66}$–$PEG_{114}$ LB films was also confirmed to be in the stable $\alpha$-helical conformation by the same spectroscopic methods.

**Molecular Orientation of the PLeu Segment in Monolayer.** Figure 4 shows the surface pressure-area ($\pi$-$A$) isotherm for monolayer of $PLeu_{80}$–$PEG_{23}$ at the air–water interface. The values on the abscissa in this case indicate the area per one block copolymer molecule. The surface pressure increased by compression from 14.0 to 11.0 nm$^2$/molecule, followed by a little plateau up to 8.0 nm$^2$/molecule and showed another increase by further compression of the monolayer from 8.0 nm$^2$/molecule. The two steep increase parts in the isotherm suggest the existence of different molecular arrangements in the monolayer. Extrapolations of each steep increase part of the isotherm to $\pi = 0$ gave two values of limiting area of $PLeu_{80}$–$PEG_{23}$ monolayer, $A_S$ and $A_L$, respectively, in Fig. 4. We similarly estimated $A_L$ and $A_S$ values for $PLeu_{57}$–$PEG_{46}$ and $PLeu_{66}$–$PEG_{114}$ monolayer systems. These values of $A_S$ and $A_L$ are shown also in Table 1. The calculated values, $A_{//}$ and $A_\perp$, in Table 1 were the area per molecule of poly(L-leucine) whose degree of polymerization is 80, 57, and 66, respectively, when they oriented parallel ($A_{//}$) and normal ($A_\perp$) to the monolayer, based on the value of area per leucine residue estimated from the limiting area of poly(L-leucine) monolayer.[16] The value of $A_L$ was smaller than that of $A_{//}$ for all systems. This indicates that $\alpha$-helical rods of PLeu are not perfectly parallel to the air–water interface around $A_L$ before the steep increase in the surface pres-

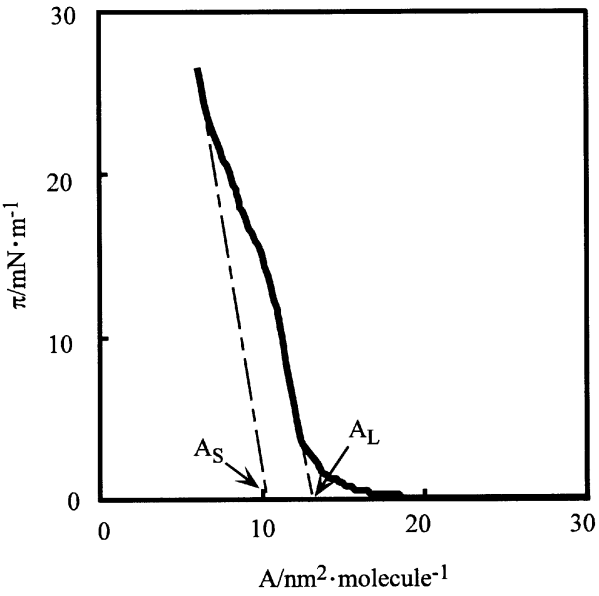


Fig. 4. $\pi$-$A$ isotherm for monolayer of $PLeu_{80}$–$PEG_{23}$.

Table 1. Limiting Area Estimated from $\pi$-$A$ Isotherms (nm$^2$/molecule)

| | Observed | | Calculated | | $A_S/A_\perp$ | $A_{PEG}$ |
|---|---|---|---|---|---|---|
| | $A_L$ | $A_S$ | $A_{//}$ | $A_\perp$ | | |
| $PLeu_{80}$–$PEG_{23}$ | 12.3 | 10.4 | 15.9 | 1.5 | 6.7 | 1.4 |
| $PLeu_{57}$–$PEG_{46}$ | 6.3 | 4.4 | 11.3 | 1.5 | 2.9 | 2.8 |
| $PLeu_{66}$–$PEG_{114}$ | 10.5 | 8.6 | 13.1 | 1.5 | 5.7 | 7.4 |

sure. The value of $A_S$ is smaller than that of $A_L$ indicating that the $\alpha$-helical segments can tilt more with respect to the interface by compression of the monolayer. It has been already confirmed that $\alpha$-helix rod of poly(L-leucine) could not stand in the monolayer at the air–water interface.[15] One may say, therefore, that the PEG segment is essential for the tilting of PLeu segment in these copolymer monolayer systems. The solubilization of the hydrophilic PEG segment into water may make the PLeu segment stand at the interface. Furthermore, we evaluated the degree of molecular orientation of PLeu by the ratio, $A_S/A_\perp$ (Table 1). As the result, the value of $A_S/A_\perp$ of $PLeu_{57}$–$PEG_{46}$ was smaller than those of other systems, indicating that there is an optimum composition for the copolymers to be effectively oriented at the air–water interface.

In order to estimate the PEG segment size, the area per molecule of PEG segment for each block copolymer was calculated based on the free-jointed chain model and this area is shown as $A_{PEG}$ in Table 1. In $PLeu_{66}$–$PEG_{114}$ system, the observed $A_S$, 8.6 $nm^2$/molecule, is comparable to $A_{PEG}$, 7.4 $nm^2$/molecule. This means, at high surface pressure region, the interaction between the large PEG segment itself may disturb the further tilting of the PLeu segment. On the other hand, the fact that $\alpha$-helix rod can not stand in the poly(L-leucine) monolayer may be due to the polypeptide helix–helix interaction which stabilizes the helix aggregated large domain structure so as to prevent tilting of individual $\alpha$-helix molecules in the monolayer. The structural stability of the $PLeu_{80}$–$PEG_{23}$ monolayer whose helix rod is parallel to the monolayer plane is almost identical with that of poly(L-leucine) monolayer, because the PEG segment is too small to prevent PLeu–PLeu interactions. This is the reason why there is an optimum chain length of PEG segment to effectively induce the normal orientation of $\alpha$-helical part at air–water interface.

We measured FT-IR/RAS of $PLeu_m$–$PEG_n$ monolayer to confirm the orientation of PLeu segment in the monolayer. In order to evaluate the orientation in the solid condensed monolayer, we transferred the monolayer onto a Au substrate at 25 mN $m^{-1}$. The spectrum of $PLeu_{57}$–$PEG_{46}$ LB (monolayer) film has been already shown in Fig. 3. As the transition moment direction with respect to the helix axis was different between Amide I and II, the tilt angle ($\gamma$) of the $\alpha$-helix rod from normal to the monolayer was estimated using Eqs. 1 and 2, and the ratio of the individual intensities of Amide I and II absorption (Table 2). It is clear that the PLeu segment tilts slightly from the perpendicular to the membrane plane in the all $PLeu_m$–$PEG_n$ monolayer systems. Furthermore, the tilt angle of $PLeu_{57}$–$PEG_{46}$ was smaller than $PLeu_{80}$–$PEG_{23}$ and $PLeu_{66}$–$PEG_{114}$ systems. This agreed with the result of $A_S/A_\perp$ in Table 1 obtained from the $\pi$-$A$ isotherm.

Table 2. $A_I/A_{II}$ Ratios and Values of Tilt Angle ($\gamma$) of $\alpha$-Helix from Normal to the Monolayer

| | $A_I/A_{II}$ | $\gamma$ |
|---|---|---|
| $PLeu_{80}$–$PEG_{23}$ | 1.60 | 53° |
| $PLeu_{57}$–$PEG_{46}$ | 2.25 | 45° |
| $PLeu_{66}$–$PEG_{114}$ | 1.44 | 62° |

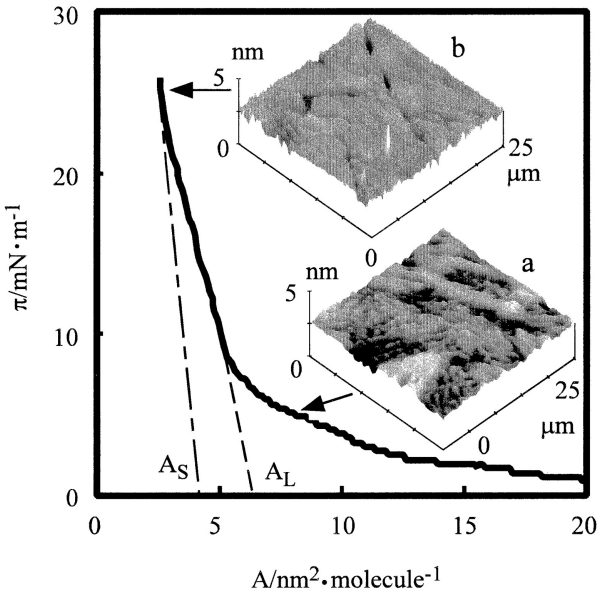


Fig. 5. $\pi$-$A$ isotherm and AFM images of $PLeu_{57}$–$PEG_{46}$.

**AFM Image of $PLeu_m$–$PEG_n$ Monolayer.** The morphology of monolayer was directly observed by atomic force microscope (AFM) using $PLeu_{57}$–$PEG_{46}$ LB films transferred by the vertical dipping method at $\pi = 5$ and 25 mN $m^{-1}$. AFM images are shown in Fig. 5 (a; 5 mN $m^{-1}$, b; 25 mN $m^{-1}$) with the $\pi$-A isotherm. It is clear that large domains of several μm in size exist in the LB (monolayer) film, in Fig. 5a, indicating a $PLeu_{57}$–$PEG_{46}$ aggregation at air–water interface even at lower surface pressure (5 mN $m^{-1}$). Figure 5b shows an AFM image of the LB film of $PLeu_{57}$–$PEG_{46}$ obtained by transferring the monolayer at 25 mN $m^{-1}$ from water surface onto the mica substrate. With the compression of the monolayer up to 25 mN $m^{-1}$, the domains assembled together to yield a condensed, rather homogeneous monolayer. However, several gaps are clearly seen along the junctions of the domains.

## Conclusion

Amphiphilic block copolymers, $PLeu_m$–$PEG_n$ ($m$:$n$ = 80:23, 57:46, 66:114), formed a stable monolayer at the air–water interface. PLeu segment maintained the $\alpha$-helical conformation in the monolayer. The $\pi$-$A$ isotherms and FT-IR/RAS measurements showed that $\alpha$-helical rods of PLeu segment tend to stand at the interface by compression of the monolayer. Thus it was confirmed that PEG segments were essential for the normal orientation of PLeu segments. However, the degree of tilting of helical rods from the surface normal was different among these three samples, i.e., there is an optimum length of PEG segment to effectively stand the $\alpha$-helical part of the amphiphiles at the air–water interface. The compression of the monolayer induced the aggregation of monolayer domains which preexisted under the lower surface pressure, and the aggregate face of the domains is left as a gap in the solid condensed state of the monolayer.

This work was partially supported by a Grant-in-Aid for the Scientific Research from the Ministry of Education, Science, Sports and Culture, and has been supported by CREST of JST (Japan Science and Technology).

## References

1 N. Unwin, *Nature*, **373**, 37 (1995).

2 H. Menzel, B. Weichart, and M. L. Hallensleben, *Thin Solid Films*, **223**, 181 (1993).

3 R. Jones and R. H. Tredgold, *J. Phys. D: Appl. Phys.*, **21**, 449 (1988).

4 E. P. Enriquez and E. T. Samulski, *Mat. Res. Soc. Symp. Proc.*, **225**, 423 (1992).

5 J. K. Whitesell and H. K. Chang, *Science*, **261**, 73 (1993).

6 J. K. Whitesell, H. K. Chang, and C. S. Whitesell, *Angew. Chem., Int. Ed. Engl.*, **33**, 871 (1994).

7 Y. Imanishi, K. Fujita, Y. Miura, and S. Kimura, *Supramol. Sci.*, **3**, 13 (1996).

8 A. Toyotama, S. Kugimiya, M. Yonese, T. Kinoshita, and Y. Tsujita, *Chem. Lett.*, **1997**, 443.

9 H. Hosokawa, T. Kinoshita, Y. Tsujita, and H. Yoshimizu, *Chem. Lett.*, **1997**, 745.

10 K. Kishihara, T. Kinoshita, T. Mori, and Y. Okahata, *Chem. Lett.*, **1998**, 951.

11 T. Kinoshita, T. Doi, A. Kato, H. Hosokawa, Y. Tsujita, and H. Yoshimizu, *Chaos*, **9**, 255 (1999).

12 K. Fujita, N. Bunjes, K. Nakajima, M. Hara, H. Sasabe, and W. Knoll, *Langmuir*, **14**, 6167 (1998).

13 T. Sakurai, T. Kinoshita, Y. Tsujita, and H. Yoshimizu, *Polym. Prepr. Jpn.*, **47**, 4105 (1998).

14 T. Doi, T. Kinoshita, Y. Tsujita, and H. Yoshimizu, *Seni Gakkai Shi*, **56**, 221 (2000).

15 N. Greenfield and G. D. Fasman, *Biopolymer*, **8**, 4108 (1969).

16 T. Yamashita, A. Shibata, and S. Yamashita, *Bull. Chem. Soc. Jpn.*, **51**, 2751 (1978).